Materials Science in Semiconductor Processing 121 (2021) 105325

Contents lists available at ScienceDirect

Materials Science in Semiconductor Processing

journal homepage: http://www.elsevier.com/locate/mssp

Calculation of characteristics parameters of Au /methyl green/*n*-Si/Ag diodes from the current-voltage measurements

F.S. Kaya [a,*], S. Duman [b], O. Baris [c], B. Gurbulak [a]

[a] *Department of Physics, Science Faculty, Ataturk University, 25240, Erzurum, Turkey*
[b] *Department of Basic Sciences, Science Faculty, Erzurum Technical University, 25050, Erzurum, Turkey*
[c] *Department of Biology, Science Faculty, Ataturk University, 25240, Erzurum, Turkey*

ARTICLE INFO

Keywords:
Methyl green
Barrier height
Ideality factor
Drop coating

ABSTRACT

In this study, methyl-green (MG) organic dye layer was formed on the front side of a *n*-Si semiconductor via low–cost drop coating method and twenty (20) Au/MG/*n*-Si/Ag diodes have been identically fabricated. The fundamental diode parameters such as barrier height (BH, $\varnothing_b$), ideality factor (IF, n) and series resistance (R_s) were determined from the current–voltage (*I–V*) measurements by using ln(*I*)–*V* characteristics, Cheung's functions and modified Norde's functions at room temperature. The values of BH and IF calculated from ln(*I*)-*V* were varied from 0.744 to 0.862 eV and from 1.10 to 1.64 for the 20 Au/MG/n-Si/Ag diodes, respectively. The experimental BH and IF distributions calculated from the ln(*I*)–*V* characteristics and Cheung's functions were fitted by a Gaussian distribution function. The statistical analysis yielded a mean IF value of 1.26 with standard deviation (σ) of 0.173 and a mean BH value of 0.817 eV with σ of 0.031 eV from the ln (*I*)–*V* characteristics, respectively. It was seen that there is an agreement between the BH values calculated from ln(*I*)-*V* and other two methods. The R_s obtained from Norde's function were compared with those from Cheung's functions.

1. Introduction

Metal–semiconductor (M-S) contacts have an important place in semiconductor technology. Since different M-S contacts have been investigated over a long period, the physics of M-S contacts is widely known. M-S contacts have applications in various electronic devices due to their low cost and easy fabrication. Many methods are used to improve the interface of M-S contacts. One of these methods is to insert an organic-dye layer between a metal and a semiconductor. Organic-dye layer affects the device performance and improve electronic properties of M-S contacts [1,2]. Organic dyes are very important for electronic circuit components. Methyl green (MG) is a molecule belonging to the triphenylmethane groups. The molecular weight of MG is 472.5 g/mol. The molecular formula of MG is $C_{26}H_{33}N_3Cl_2$ and its molecular structure is given in Fig. 1.

In our previous studies, Al/MG/*p*-Si structure with the ideality factor (IF) value of 1.36 and the barrier height (BH $\varnothing_b$) of 0.80 eV and Al/MG/*p*-Ge structure with the IF value of 1.14 and BH of 0.82 eV were fabricated using Al metal with a work function of 4.28 eV [2,3].

The aim of this study is to fabricate Au/MG/*n*-Si/Ag diode, to provide variation of BH value for Au/*n*-Si diode by inserting the MG organic dye layer between Au (with 5.1 eV work function [4]) and *n*-Si semiconductor and to calculate its diode characteristics (BH, IF, R_s) by using different methods. According to our knowledge, the various organic layers coated on the *n*-Si semiconductor are already given in literature, but such information for Au/MG/*n*-Si/Ag is not given in the literature.

2. Experimental

The diodes were prepared using *n*-Si (100) semiconductor with 5–10 Ω cm resistivity. The *n*-Si sample was divided into two pieces and one piece was used to fabricate reference diode. The cleaning procedure of *n*-Si sample was given in Refs. [5]. After the cleaning procedure of *n*-Si samples, silver (Ag) metal was evaporated to the back surface of the cleaned *n*-Si samples to form ohmic contact. Then *n*-Si/Ag samples was annealed at 420 °C for 3 min in a pure N_2 atmosphere. 0.1 g of MG was dissolved in 10 ml of methyl alcohol and kept light-free manner. The MG organic dye layer was formed via low–cost drop coating method on the bright surface of other piece of *n*-Si and left to dry. Gold (Au) metal (99.99% purity) was evaporated both samples with metal shadow mask of 1.0 mm diameter at a pressure of 10^{-6} Torr. Thus the Au/*n*-Si/Ag reference diode and the 20 Au/MG/*n*-Si/Ag diodes were identically

* Corresponding author.
E-mail address: fs_ozcelik@hotmail.com (F.S. Kaya).

https://doi.org/10.1016/j.mssp.2020.105325
Received 3 February 2020; Received in revised form 18 May 2020; Accepted 8 July 2020
Available online 28 July 2020
1369-8001/

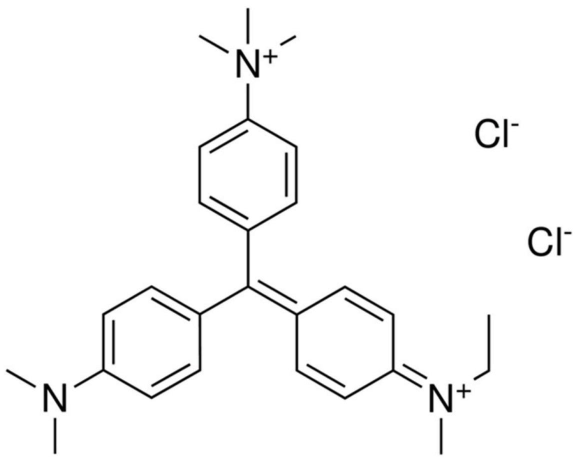

Fig. 1. Molecular structure of MG.

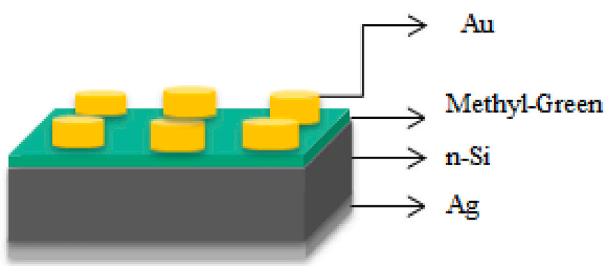

Fig. 2. (Colour online) Schematic diagram of the Au/MG/*n*-Si/Ag diodes.

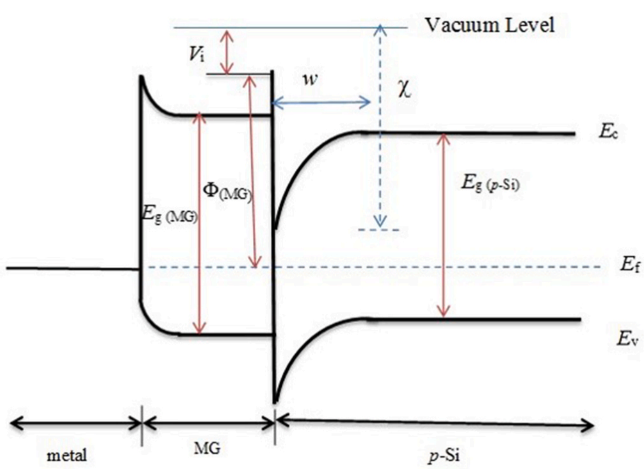

Fig. 3. (Colour online) The energy band diagram of MG/*p*-Si diode.

fabricated. The current–voltage (*I*–*V*) measurements were carried out using a Keithley 2400 Picoammeter/Voltage source at room temperature. Fig. 2 shows a schematic diagram of the Au/MG/*n*-Si/Ag diode.

3. Results and discussion

Figs. 3 and 4 show energy band diagrams of MG/*p*-Si and MG/*n*-Si diodes in thermal equilibrium , respectively. $E_{g\,(MG)}$ is the band gap of the MG, $E_{g\,(Si)}$ is the band gap of Si semiconductor, E_f is the Fermi energy level, $\Phi_{(MG)}$ is the work function of the MG, V_i is the potential drops across the interfacial layer, w is the width of the depletion region, χ is the electron affinity of the Si semiconductor [6–11].

Fig. 5 shows ln(*I*)-*V* characteristic of the Au/*n*-Si/Ag reference diode

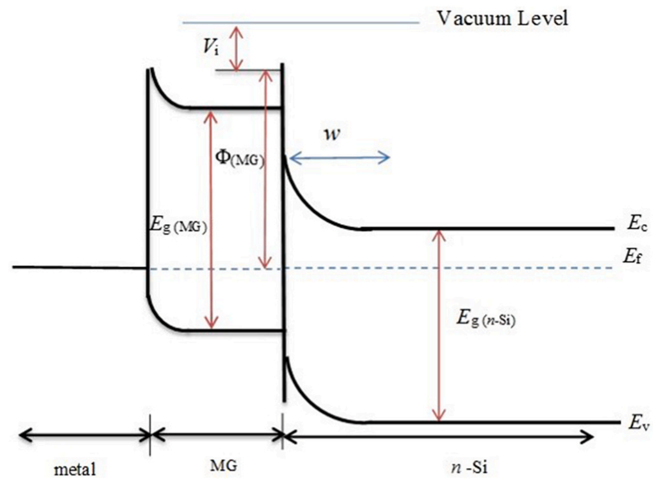

Fig. 4. (Colour online) The energy band diagram of MG/*n*-Si diode.

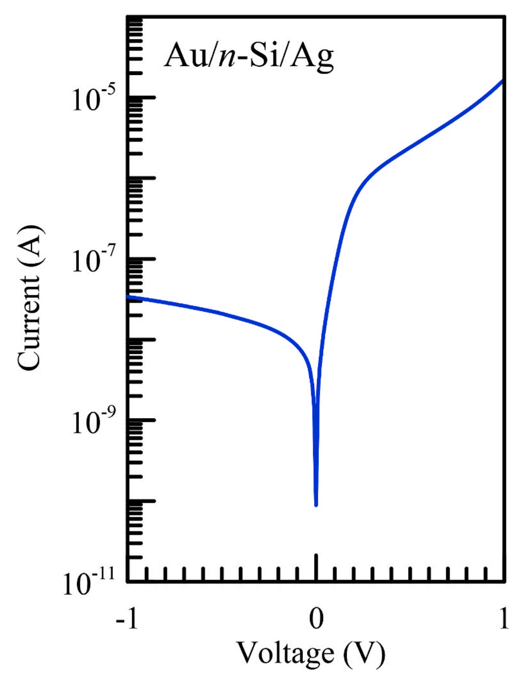

Fig. 5. (Colour online) The *I-V* characteristic of the Au/*n*-Si/Ag diode in the dark.

in the dark. The values of BH and IF *of* the Au/*n*-Si/Ag diode were calculated as 1.33 and 0.791 eV from the *y*-axis intercept and slope of the linear region of the experimental forward bias ln(*I*)-*V* data, respectively.

The ln(*I*)-*V* characteristics of the Au/MG/*n*-Si/Ag diodes are given in Fig. 6. As can be seen from Fig. 6, the ln(*I*)-*V* characteristics of the Au/MG/*n*-Si/Ag diodes show the rectifying behavior and the reverse bias curves exhibit a good saturation. While the Au/*n*-Si/Ag diode has a 5×10^2 of rectification ratio (RR), the Au/MG/*n*-Si/Ag diodes have RR between about 3×10^2 and 6×10^5 at ± 1 V. Thus a RR as high as 10^5 was achieved for the 11 Au/MG/*n*-Si/Ag diodes.

Fig. 7 presents the ln(*I*) -*V* characteristics of the selected 5 Au/MG/*n*-Si/Ag diodes under dark and light illumination conditions. The forward bias current remains unchanged while the reverse bias current increases by the light illumination. Since MG layer absorbs visible light, the generation of free carriers effectively increases the reverse current value compared to the dark current [3,12].

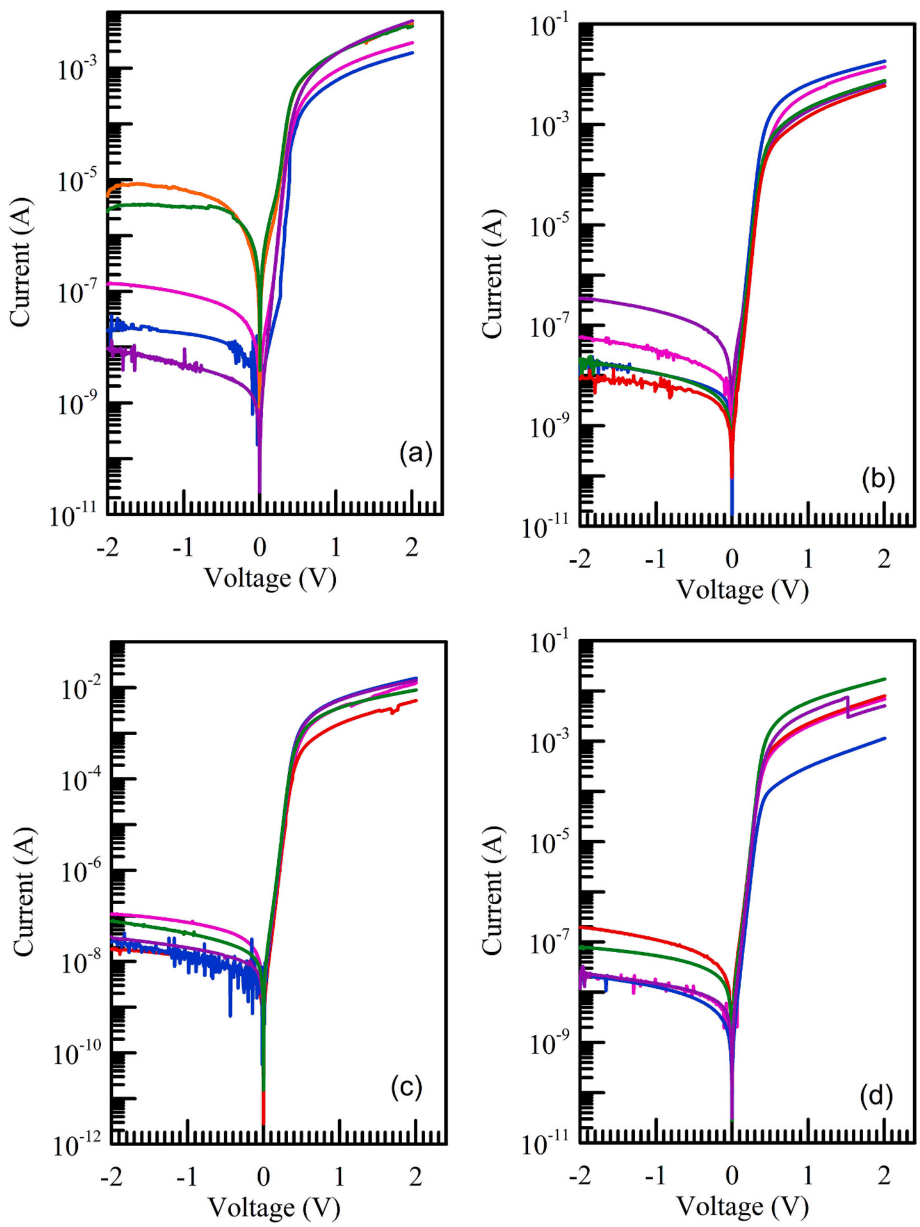

Fig. 6. (Colour online) The *I-V* characteristics of the Au/MG/*n*-Si/Ag diodes (a) 1 to 5, (b) 6 to10, (c) 11 to 15, and (d) 16 to 20.

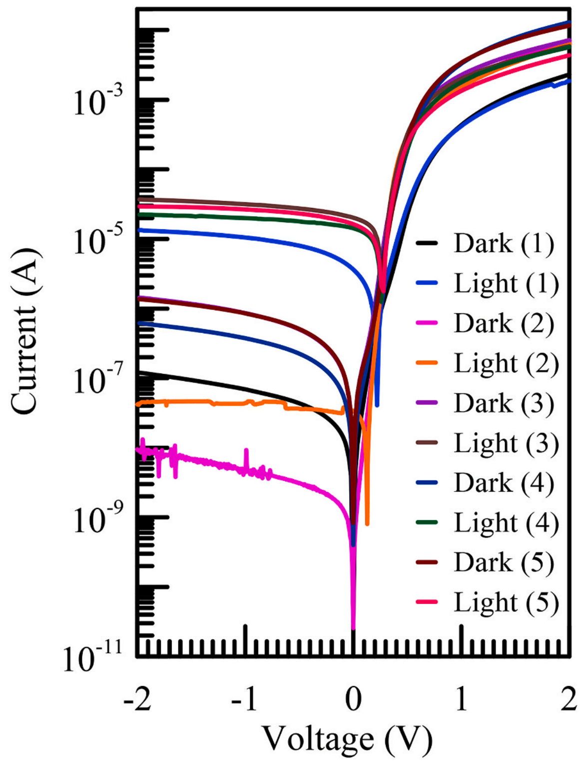

Fig. 7. (Colour online) The ln(*I*)–*V* characteristics of the selected 5 Au/MG/*n*-Si/Ag diodes under dark and light illumination conditions.

The IF and BH values of the Au/MG/*n*-Si/Ag diodes were calculated to thermionic emission (TE) theory from the ln(*I*)–*V* characteristics [10–15]. The experimental distribution of the BHs and IFs were fitted by a Gaussian function. The value of BH and IF varied from one diode to another even if they were identically prepared [16].

Fig. 8 (a) and (b) shows histograms of the IF and BH values of the Au/MG/*n*-Si/Ag diodes. The IF and BH values of the Au/MG/n-Si/Ag diodes are in the range of 1.10–1.64 and 0.744–0.862 eV, respectively. The IF values of the 12 Au/MG/n-Si/Ag diodes are lower than the value of 1.20. The Gaussian fits yielded a mean IF value of 1.26 with standard deviation (σ) of 0.173 (Fig. 8a) and a mean BH value of 0.817 eV with σ of 0.031 eV (Fig. 8b) for the Au/MG/*n*-Si/Ag diodes. This value of mean BH is higher than that of reference Au/n-Si/Ag diode. The Au/MG/n-Si/Ag diodes show organic-on-inorganic semiconductor heterojunction behavior. The potential barrier exists at the interface between the organic MG and *n*-Si inorganic semiconductor. This potential barrier controls the injection of charge from the Au/MG contact into the inorganic *n*-Si semiconductor. In reverse bias (i.e. where the Ag back ohmic contact is at a positive potential relative to the Au top contact on the MG layer), the carriers must overcome the potential barrier. Under forward bias, the carriers are injected from the *n*-Si semiconductor into the organic MG layer [16–20].

The curve of BH *vs.* IF of the Au/MG/*n*-Si/Ag diodes was presented in Fig. 9. The values of BH become smaller as the values of IF increase. The linear relation between IF and BH in structure can be explained by lateral inhomogeneities [21,22]. The value of BH was calculated 0.847 eV for $n = 1$ from extrapolation of BH *vs.* IF curve given in Fig. 9.

The BH and IF values of various diodes fabricated using *n*-Si semiconductor in literature were given in Table 1. The mean BH value of 0.817 eV obtained for the Au/MG/*n*-Si/Ag diodes is higher than the calculated BH value for the conventional Au/*n*-Si diode [6,23,24] and than most of the values [20,25,27,28,30–34,37–41] given in Table 1 for the metal/organic material/*n*-Si structures. Furthermore, the mean IF value of 1.26 is lower than most of the values [20,24–41] given in Table 1.

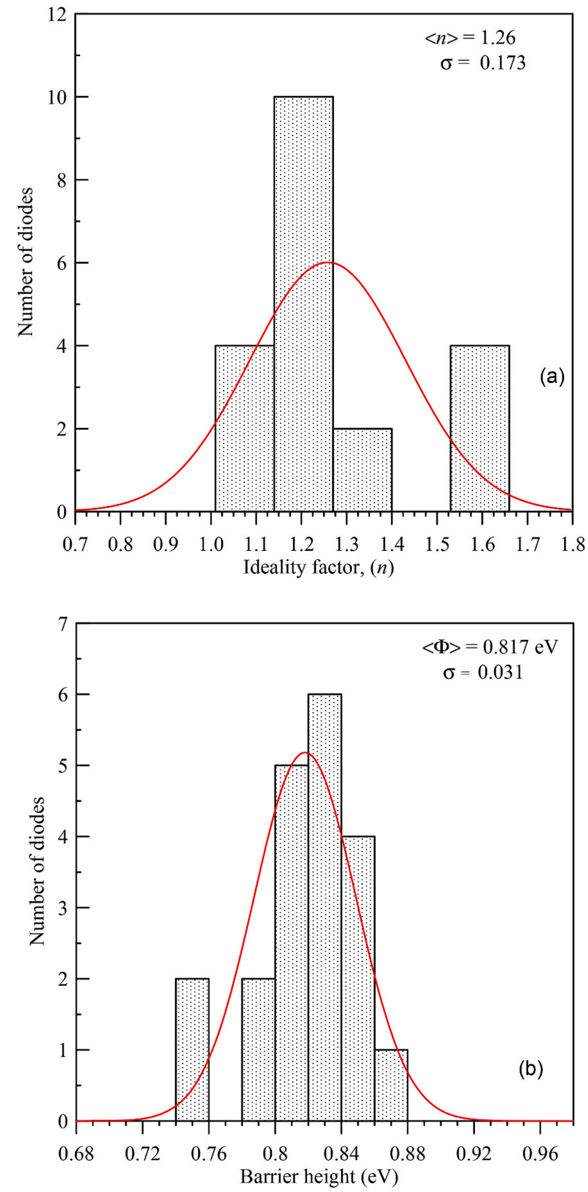

Fig. 8. (Colour online) The Gaussian distribution of (a) IFs and (b) BHs calculated from the ln(*I*)–*V* characteristics of the Au/MG/*n*-Si/Ag diodes.

The forward bias ln(*I*)–*V* characteristics of the Au/MG/*n*-Si/Ag diodes deviate from linearity due to the effect of series resistance (R_s). Beside the conventional *I*–*V* curves, Cheung's methods [42,43] are used to determine the R_s and BH ($\varnothing_b$) values of the Au/MG/*n*-Si/Ag diodes. The values of the IF and R_s can be determined from the following equations:

$$\frac{dV}{d(\ln I)} = \frac{nkT}{q} + IR_s \tag{1}$$

A plot of $\frac{dV}{d(\ln I)} - I$ should be straight line. The slope and y-axis intercept of this plot will give R_s and $\frac{nkT}{q}$ using Eq. (1), respectively. A plot of $H(I) - I$ function is used to calculate the values of the BH and R_s.

$$H(I) = V - \left(\frac{nkT}{q}\right)\ln\left(\frac{I}{AA^{*}T^{2}}\right) \tag{2}$$

$$H(I) = n\phi_b + IR_s \tag{3}$$

Fig. 10 shows the $\frac{dV}{d(\ln I)} - I$ and $H(I) - I$ plot of the diode 7. The various

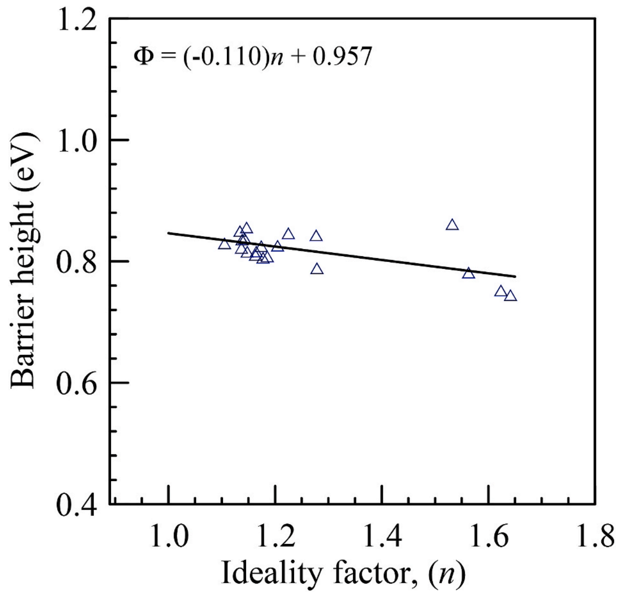

Fig. 9. (Colour online) The curve of BH *vs* IF of the Au/MG/*n*-Si/Ag diodes.

Table 1
The BH and IF values of metal/*n*-Si diodes with and without interfacial layer.

Diode	*BH* (eV)	IF	Ref.
Au/*n*-Si/Ag	0.791	1.33	Present work
Au/*n*-Si	0.803	1.10	[6]
Au/*n*-Si	0.790	1.25	[23]
Au/*n*-Si	0.510	4.43	[24]
Al/methyl violet (MV)/*n*-Si/AuSb	0.780	3.38	[20]
Ag/β-caroten/*n*-Si	0.800	1.32	[25]
Au/chitin/*n*-Si	0.959	1.55	[26]
Sn/rhodamine-101/*n*-Si	0.714	2.72	[27]
Al/newfuchsin/*n*-Si	0.800	3.14	[28]
Au/1,1-dimethylferrocenecarboxylate/*n*-Si	0.830	1.54	[29]
Cr/*n*-Si/Au-Sb	0.316	2.25	[30]
PVA (Bi2O3-doped)Au/*n*-Si	0.740	3.49	[31]
Au/(PVA)/*n*-Si:Co,Zn	0.750	1.80	[32]
Au/polyvinyl alcohol (PVA)/*n*-Si:Bi	0.730	3.98	[33]
Au/perylenemonoimide/*n*-Si	0.675	5.08	[34]
Au/TiO2/*n*-Si	0.820	1.92	[35]
Au/(PVA)/*n*-Si:Bi	0.920	2.06	[36]
Au/Si3N4/*n*-Si	0.740	3.43	[37]
Au/(PVA)/*n*-Si:Co	0.710	1.40	[38]
Perylene-monoimide/*n*-Si	0.694	4.27	[39]
Au/perylene-diimide/*n*-Si	0.690	1.57	[40]
Grafen/Si-pillar junction	0.110	2.60	[41]

parameters calculated from Cheung's functions were given in Table 2.

The IF and BH values of the Au/MG/*n*-Si/Ag structure obtained from Cheung's functions were shown in Figs. 11 and 12. The Gaussian fits yielded a mean IF value of 1.37 with σ of 0.226 (Fig. 11) and a mean BH value of 0.790 eV with σ of 0.038 eV (Fig. 12) for the Au/MG/*n*-Si/Ag diodes. The values of IF obtained from the ln(*I*)-*V* and d*V*/*d*(*lnI*) characteristics are different from each other. This difference can be attributed to the existence of the R_s. Also, the R_s values obtained from the(d*V*/*d*(ln*I*)-*I*) and *H*(*I*)-*I* curves are in agreement with each other.

The values of BH (Φ_b) and R_s were calculated from Norde's function [44] *F*(V) by using Eqs. (4) and (5), respectively.

$$\Phi_b = F(V_{min}) + \left[\left(\frac{\gamma - n}{n}\right)\right]\left[\frac{V_{min}}{\gamma} - \frac{kT}{q}\right] \tag{4}$$

$$R_s = \frac{(\gamma - n)kT}{qI_{min}} \tag{5}$$

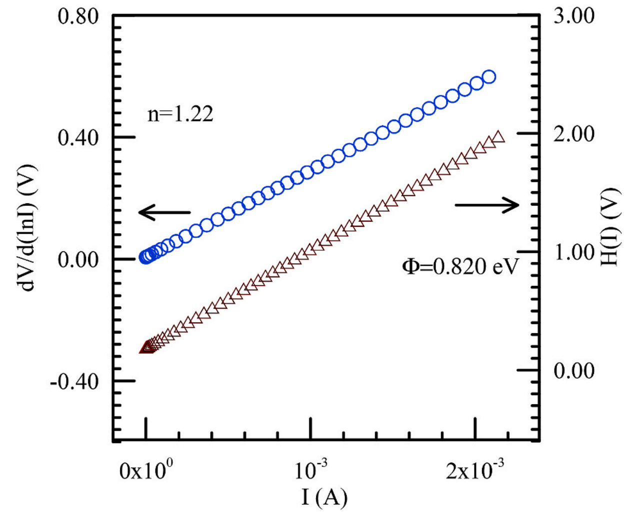

Fig. 10. (Colour online) A plot of *H*(*I*) and *dV*/*d*(*lnI*) versus *I* for the diode 7.

Table 2
The values of IF, BH, and R_s calculated from ln (*I*)-*V* characteristics and Cheung's functions for the Au/MG/*n*-Si/Ag diodes.

Diode Number	*IF (ln (I)-V)*	BH (eV) (*ln(I)-V*)	R_s (Ω) (d*V*/*d* (*lnI*)-I)	IF (d*V*/*d* (*lnI*)-*I*)	R_s (Ω) *H*(*I*)-*I*	BH (eV) *H*(*I*)-*I*
1	1.53	0.862	913	1.60	683	0.833
2	1.28	0.843	602	1.52	562	0.802
3	1.62	0.752	320	1.80	279	0.718
4	1.64	0.744	326	1.81	290	0.708
5	1.22	0.846	272	1.51	265	0.810
6	1.15	0.856	362	1.60	315	0.790
7	1,14	0,836	266	1,22	255	0.820
8	1,13	0,850	121	1,30	120	0.826
9	1.56	0.782	283	1.57	264	0.773
10	1.15	0.816	92	1.35	89	0.755
11	1.19	0.808	106	1.36	268	0.810
12	1.20	0.826	374	1.16	352	0.827
13	1.16	0.811	183	1.50	175	0.710
14	1.14	0.822	115	1.18	110	0.794
15	1.17	0.825	156	1.03	164	0.844
16	1.10	0.829	304	1.21	285	0.805
17	1.28	0.789	287	1.12	268	0.801
18	1.18	0.806	105	1.09	100	0.800
19	1.16	0.816	150	1.32	145	0.786
20	1.14	0.838	2230	1.15	2023	0.793

Fig. 13 shows the $F(V) - V$ and $H(I) - I$ plot of the diode 7. The values of R_s and BH calculated from Norde's functions were given in Table 3.

As can be seen from Tables 2 and 3, there is an agreement between the values of BH obtained from the forward bias ln (*I*)-*V*, Cheung's and Norde's functions for the Au/MG/*n*-Si/Ag diodes. The value of *Rs* obtained from Norde's functions is lower than that of Cheung's functions. Cheung's functions are only applied to the high voltage region of the forward biased ln(*I*)–*V* characteristic but Norde's function is applied to full the forward biased ln (*I*)–*V* characteristic of diode.

4. Conclusion

The organic dye layer (MG) was formed between Au and *n*-Si semiconductor and the 20 Au/MG/*n*-Si/Ag diodes were fabricated. Then the *I*–*V* measurement of the diodes was performed. The MG organic dye layer on the *n*-Si substrate showed a good rectifying behavior. The values of IF, BH, and R_s were calculated using ln (*I*)–*V* characteristics, Cheung's functions and Norde's functions. The IF calculated from ln (*I*)–

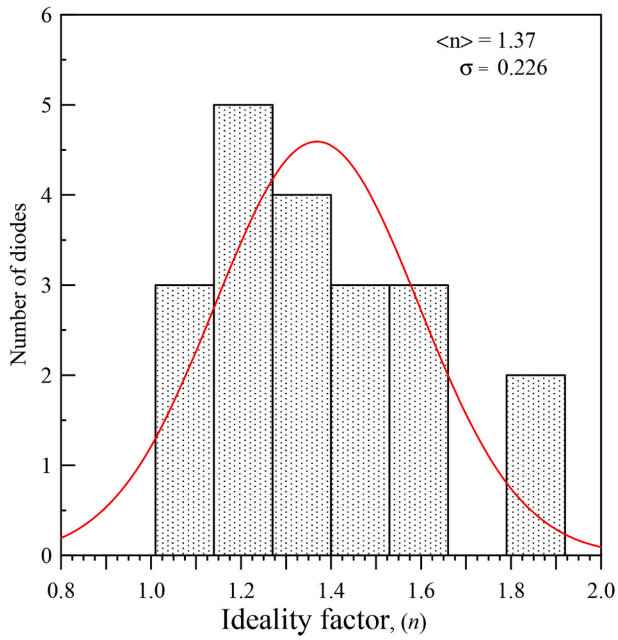

Fig. 11. The Gaussian distribution of IF values obtained from the Cheung's functions of the Au/MG/n-Si/Ag diodes.

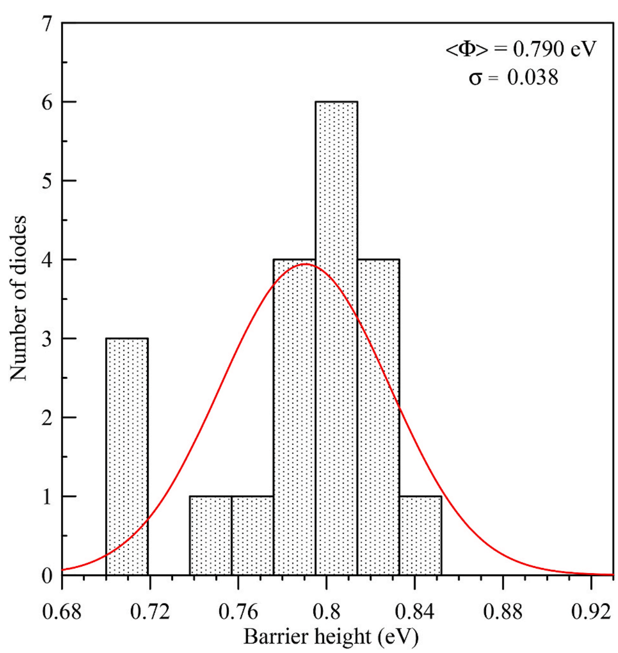

Fig. 12. The Gaussian distribution of BHs obtained from the Cheung's functions of the Au/MG/n-Si/Ag diodes.

V characteristics varied from 1.10 to 1.64 and BH was between 0.744 and 0.862 eV, respectively. The mean BH value of 0.817 eV obtained for the diodes with the organic MG layer is higher than that of the Au/n-Si diode. Morever, the mean IF value of 1.26 calculated for Au/MG/n-Si/Ag diodes is lower than most of the values given in Table 1 for the metal/organic compound/inorganic semiconductor diodes. Thus MG thin film interface layer coated with drop-coating on n-Si can be used as an alternative to other highly expensive and difficult methods and for obtaining diodes with higher BH.

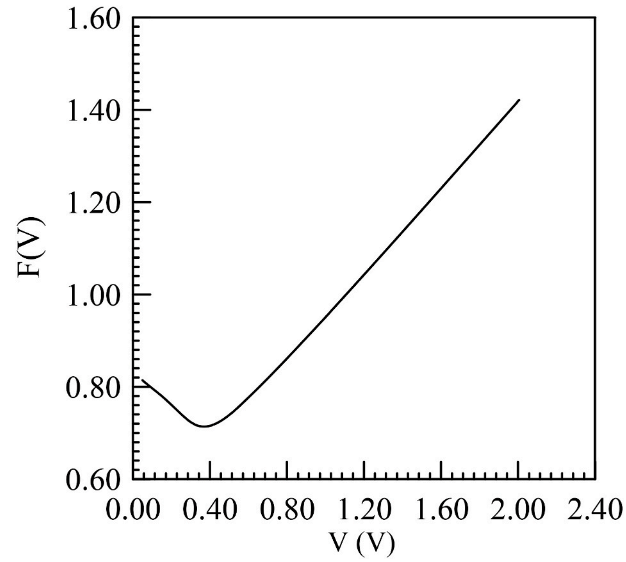

Fig. 13. A plot of $F(V) - V$ for the diode 7.

Table 3
The values of BH and R_s calculated from Norde's functions for the 20 Au/MG/n-Si/Ag diodes.

Diode Number	BH (eV)	R_s (Ω)	V(V)	F(V)	I(A)
1	0.811	402	0.395	0.759	3.01×10^{-5}
2	0.836	525	0.375	0.744	3.56×10^{-5}
3	0.744	82.1	0.365	0.708	1.19×10^{-4}
4	0.740	88.7	0.355	0.707	1.04×10^{-4}
5	0.841	331	0.385	0.736	6.06×10^{-5}
6	0.847	315	0.375	0.727	6.99×10^{-5}
7	0.835	210	0.370	0.714	1.06×10^{-4}
8	0.847	244	0.380	0.722	9.18×10^{-5}
9	0.769	143	0.375	0.724	7.88×10^{-5}
10	0.810	63.1	0.380	0.688	3.49×10^{-4}
11	0.803	66.6	0.380	0.690	3.16×10^{-4}
12	0.827	163	0.385	0.717	1.26×10^{-4}
13	0.805	115	0.360	0.694	1.88×10^{-4}
14	0.819	81.8	0.380	0.694	2.73×10^{-4}
15	0.822	127	0.380	0.707	1.68×10^{-4}
16	0.828	205	0.355	0.705	1.13×10^{-4}
17	0.780	116	0.355	0.695	1.61×10^{-4}
18	0.798	50.7	0.380	0.683	4.20×10^{-4}
19	0.809	138	0.360	0.699	1.57×10^{-4}
20	0.848	882	0.345	0.738	2.51×10^{-5}

Declaration of competing interest

The authors have no affiliation with any organization with a direct or indirect financial interest in the subject matter discussed in the manuscript.

References

[1] M. Zhu, J. Zhang, H. Hou, Microelectron. Eng. 95 (2012) 112–115.
[2] S. Duman, F.S. Ozcelik, B. Gurbulak, M. Gulnahar, A. Türüt, Metall. Mater. Trans. 46A (2014) 347–353.
[3] S. Duman, G. Turgut, F.S. Ozcelik, B. Gurbulak, Philos. Mag. A 95 (2015) 1646–1655.
[4] K. Shimura, H. Yoshida, Energy Environ. Sci. 4 (2011) 2467–2481.
[5] G. Turgut, S. Duman, F.S. Ozcelik, Metall. Mater. Trans. 48A (2017) 3137–3142.
[6] S. Mahato, J. Puigdollers, Phys. B Condens. Matter 530 (2018) 327–335.
[7] D.Y. Khang, J. Phys. D Appl. Phys. 52 (2019), 503002.
[8] R.K. Gupta, M.E. Aydın, F. Yakuphanoglu, Synth. Met. 161 (2011) 2355–2360.
[9] M. Pietsch, M. Bashouti, S. Christiansen, J. Phys. Chem. C 117 (2013) 9049–9055.
[10] O. Gullu, M. Cankaya, M. Biber, A. Turut, J. Phys. Condens. Matter 20 (2008), 215210 (6pp).
[11] M. Soylu, F. Yakuphanoglu, Superlattice. Microst. 52 (2012) 470–483.
[12] F. Yakuphanoglu, Sol. Energy Mater. Sol. Cells 91 (2007) 1182–1186.

[13] R.F. Schmitsdorf, T.U. Kampen, W. Mönch, J. Vac. Sci. Technol., B 15 (1997) 1221.
[14] S. Duman, S. Dogan, B. Gurbulak A. Turut, Appl. Phys. A 91 (2008) 337–340.
[15] M. Biber, O. Gullu, S. Forment, R.L. Van Meirhaeghe, A. Turut, Semicond. Sci. Technol. 21 (2006) 1–5.
[16] W. Mönch, J. Vac. Sci. Technol., B 17 (1999) 1867–1876.
[17] M. Çakar, C. Temirci, A. Türüt, Synth. Met. 142 (2004) 177–180.
[18] C. Temirci, M. Çakar, A. Türüt, Y. Onganer, Phys. Status Solidi 201 (2004) 3077–3086.
[19] R.K. Gupta, M.E. Aydın, F. Yakuphanoglu, Synth. Met. 161 (2011) 2355–2360.
[20] S. Aydogan, O. Gullu, A. Turut, Phys. Scripta 79 (2009), 035802 (6pp).
[21] W. Mönch, Phys. Rev. B 37 (1988) 7129.
[22] S. Duman, B. Gürbulak, S. Doğan, A. Türüt, Microelectron. Eng. 86 (2009), 106.
[23] R. Sharma, IEEE J. Electron. Devi. 8 (2010) 286–292.
[24] A. Tataroglu, Chin. Phys. B 22 (2013), 068402.
[25] M.E. Aydın, T. Kılıçoğlu, K. Akkılıç, H. Hoşgören, Phys. B Condens. Matter 381 (2006) 113–117.
[26] K. Akkılıç, M.E. Aydın, I. Uzun, T. Kılıçoğlu, Synth. Met. 156 (2006) 958–962.
[27] M. Çakar, N. Yıldırım, Ş. Karataş, C. Temirci, A. Türüt, J. Appl. Phys. 100 (2006), 074505 (6pp).
[28] Ö. Güllü, S. Asubay, Ş. Aydoğan, A. Türüt, Physica E 42 (2009) 1411–1416.
[29] M.E. Aydın, F. Yakuphanoğlu, G. Öztürk, Synth. Met. 160 (2010) 2186–2190.
[30] Ö. Demircioğlu, Ş. Karataş, N. Yıldırım, Ö.F. Bakkaoğlu, Microelectron. Eng. 88 (2011) 2997–3002.
[31] M. Gökçen, T. Tunç, Ş. Altındal, İ. Uslu, Curr. Appl. Phys. 12 (2011) 525–530.
[32] İ. Dökme, Ş. Altındal, İ. Uslu, J. Appl. Polym. Sci. 125 (2011) 1185–1192.
[33] S. Demirezen, Z. Sönmez, U. Aydemir, Ş. Altındal, Curr. Appl. Phys. 12 (2011) 266–272.
[34] Ö.F. Yüksel, M. Kuş, N. Şimşir, H. Şafak, M. Şahin, E. Yenel, J. Appl. Phys. 110 (2011), 024507 (7pp).
[35] B. Kınacı, S.Ş. Çetin, A. Bengi, S. Özcelik, Mater. Sci. Semicond. Process. 15 (2012) 531–535.
[36] S. Demirezen, Ş. Altındal, İ. Uslu, Curr. Appl. Phys. 13 (2012) 53–59.
[37] F.Z. Pür, A. Tataroğlu, Phys. Scripta 86 (2012), 035802 (7pp).
[38] M. Gökçen, T. Tunç, Ş. Altındal, İ. Uslu, Mat. Sci. Eng. B-Adv. 177 (2012) 416–420.
[39] N. Tuğluoğlu, S. Karadeniz, Curr. Appl. Phys. 12 (2012) 1529–1535.
[40] Ö.F. Yüksel, N. Tuğluoğlu, H. Şafak, Z. Nalçalıgil, M. Kuş, S. Karadeniz, Thin Solid Films 534, 2012, pp. 614–620.
[41] G. Luongo, A. Grillo, F. Giubileo, L. Iemmo, M. Lukosius, C. Alvarado Chavarin, C. Wenger, A. Di Bartolomeo, Nanomaterials 9 (2019) 659 (10pp).
[42] S.K. Cheung, ve N.W. Cheung, Appl. Phys. Lett. 49 (1986) 85–87.
[43] S. Duman, Z. Elkoca, B. Gürbulak, T. Tekle Bahtıyarı, S. Doğan, J. Optoelectron. Adv. Mater. 14 (2012) 693–698.
[44] H. Norde, J. Appl. Phys. 50 (1979) 5052–5053.